Journal of Atmospheric and Solar-Terrestrial Physics 94 (2013) 34–40

Contents lists available at SciVerse ScienceDirect

Journal of Atmospheric and Solar-Terrestrial Physics

journal homepage: www.elsevier.com/locate/jastp

Effect of prompt penetration on the low latitude *ASY* indices

Anand K. Singh *, A.K. Sinha, B.M. Pathan, R. Rajaram, Rahul Rawat

Indian Institute of Geomagnetism, Kalamboli Highway, New Panvel (W), Navi Mumbai 410218, Maharashtra, India

ARTICLE INFO

Article history:
Received 27 April 2012
Received in revised form
2 November 2012
Accepted 21 December 2012
Available online 11 January 2013

Keywords:
Prompt penetration
Substorm
Auroral electrojet
Asymmetry

ABSTRACT

Onset of a geomagnetic substorm often intensifies the westward auroral electrojet, as well as produces asymmetric magnetic field at low-/mid-latitudes. Auroral electrojet and low latitude asymmetric indices are known to correlate well during substorms. These indices have been widely used to monitor the duration and strength of substorm activities. However, several processes, other than substorms, introduce local time asymmetry in magnetic field at low latitudes, which can substantially influence the *ASY* indices. Large number of substorms are observed in association with changes in the interplanetary magnetic field (IMF). It is known that sharp IMF *Bz* orientation changes result in penetration of interplanetary electric field (IEF) to lower latitudes, which affects the geomagnetic fields to different degree in different local times. In the present study, we demonstrate that sharp IMF *Bz* fluctuations during the expansion phases of substorms introduce additional asymmetry at low latitudes. The effect is clearly seen in *ASYH*, whereas *ASYD* remains almost unaltered.

1. Introduction

A geomagnetic substorm is one of the most important phenomena in the solar–terrestrial relationship. It involves many interesting physical processes of magnetospheric dynamics and plays a key role in the solar wind energy dissipation into the Earth's magnetosphere and ionosphere (Akasofu, 1981; Rostoker et al., 1980). Substorms often initiate at auroral latitudes on the nightside of the Earth, but cast almost global effects in magnetic and electric observations (McPherron et al., 1973a; Huang et al., 2004; Sastri, 2002).

Davis and Sugiura (1966) introduced auroral electrojet indices (*AU*, *AL*, and *AE*) to monitor substorms, which are based on *H* disturbances observed at auroral latitudes in different local times. The westward auroral electrojet, represented by the *AL* index, is closely related to the substorm activity. Therefore, *AL* index is believed as a better indicator of substorms than *AU* or *AE* indices (Kamide and Rostoker, 2004).

During a substorm, low-/mid-latitude geomagnetic disturbances are strongly asymmetric in local time due to dominance of various current systems, such as substorm current wedge, asymmetric ring current, and ionospheric currents (Iyemori and Rao, 1996). The asymmetries in global *H* and *D* component disturbances (respectively in magnetic north–south and east–west directions) are derived using low-/mid-latitude magnetic data to indicate the effects of above-mentioned current systems. The asymmetry in *H* component is represented by the *ASYH* index, whereas the same for *D* component is given by the *ASYD* index.

Sharp intensification of auroral electrojets (depression in *AL* index) is often accompanied with rather smooth positive bay in *ASY* indices during isolated, as well as storm-time substorms (Crooker, 1972; Iyemori and Rao, 1996; Grafe et al., 1997; Wada et al., 1998). It has been recently reported by Singh et al. (2011, 2012a) that on occasions when substorms are localized poleward of the standard auroral oval and consequently not identified in the standard auroral electrojet indices, *ASY* indices could monitor such substorms. However, earlier studies show that *ASY* indices are very likely to be affected by other processes that may not be directly related to the substorm phenomenon, for example, solar wind pressure enhancements (Shi et al., 2005, 2006), asymmetric ring current during main phases of storms (Hamilton et al., 1988; Liemohn et al., 2001), generation of ionospheric current due to solar flares (Singh et al., 2012b), etc.

It is known that substorms can get triggered either in association with changes in components of the IMF (Caan et al., 1975; Lyons, 1996; Lyons et al., 1997; Troshichev et al., 1986) or solar wind variations (Kokubun et al., 1977) or even due to internal plasma instabilities (Henderson et al., 1996; Lui, 2004). The externally triggered substorms can be observed in some cases when IMF *Bz* quickly turns to north or becomes less negative after a sustained southward condition (Lyons et al., 1997; Liu et al., 2011). Hsu and McPherron (2004, 2009) showed that the magnitude of the *AL* index is higher for externally triggered substorms than those initiated spontaneously (or internally).

The inner magnetosphere of the Earth is generally shielded from the interplanetary electric field, IEF ($Esw = -V \times Bz$) or the

* Corresponding author. Tel.: +91 22 27484054.
E-mail addresses: akumars11@gmail.com, singhaaks@gmail.com (A.K. Singh).

1364-6826/$ - see front matter © 2013 Elsevier Ltd. All rights reserved.
http://dx.doi.org/10.1016/j.jastp.2012.12.015

magnetospheric electric field due to the polarization electric field associated with charge separation in the ring current region (Baumjohann and Treumann, 1997). However, there are numerous experimental evidences that the shielding can be weakened or broken on occasions (e.g., sharp and prominent changes in the orientation of IMF *Bz*) and the IEF or the magnetospheric electric field can instantly penetrate up to equatorial latitudes (Nishida, 1968; Fejer et al., 1979; Gonzales et al., 1979; Kelley et al., 1979; Kikuchi and Araki, 1979; Kikuchi et al., 2000; Sastri et al., 2001, etc.).

Sudden and prominent southward turning of IMF *Bz* frequently results in a dawn-to-dusk electric field in the inner magnetosphere (so-called undershielding), which is westward on the night side and eastward on the day side (Huang et al., 2005; Rastogi et al., 2010). The abrupt northward turning of IMF *Bz* after a prolonged southward orientation (or even significant decrease in the magnitude of southward *Bz*) produces dusk-to-dawn electric field (so-called overshielding) resulting in an eastward electric field in the night side and a westward electric field on the day side (Kelley et al., 1979; Rastogi et al., 2010). The penetration electric fields may significantly alter the dynamics of different ionospheric regions. Based on the direct observations of the ionosphere, several studies have clearly established various characteristics and consequences of the penetration electric field, e.g., local time dependence (Sastri et al., 1997), ionospheric plasma drift (Abdu et al., 1998), altitudinal changes in the ionospheric regions (Sobral et al., 1997), etc.

Ground-based magnetic field observations have also played a vital role in the study of penetration electric fields (e.g., Nishida, 1968; Veenadhari et al., 2010). Particularly, high conductivity (σ) in the E-region (~ 100 km height) of the day side ionosphere results in significant enhancement of ionospheric current ($\vec{J} = \sigma \vec{E}$, where $\vec{E}$ is the penetration electric field) thereby changing the geomagnetic field values dramatically. Relatively weaker geomagnetic effect is observed on the night side due to lower ionospheric conductivity. The effects of penetration electric fields are mainly observed in the *H* component due to the zonal ionospheric currents (Abdu et al., 2007). As discussed above, the westward (eastward) electric field on the night (day) side associated with southward turnings of IMF *Bz* would weakly depress (greatly enhance) the low latitude *H* component. Opposite effects are observed during abrupt northward turning of *Bz*, i.e., weak enhancement in *H* component on the night side and sharp depression on the dayside. It suggests that sharp and prominent orientation changes of IMF *Bz* may act as an additional feed for low-/mid-latitude asymmetry in addition to substorm associated current system.

In this paper we investigate whether sharply varying IMF *Bz* conditions affect the low latitude *ASY* indices during magnetic substorms and how well the two types of indices (*AL* and *ASY*) are correlated during smoothly and sharply varying IMF *Bz* conditions. In Section 2 of this paper, we present details of data set and method used in the study. Observational results and discussion are given Section 3. We summarize and conclude our finding in Section 4.

2. Data set and method

The geomagnetic activity indices (*AL*, *ASY*, *SYM* and *Dst*) are obtained from World Data Centre (WDC) for Geomagnetism, Kyoto. Ground magnetic field data have been taken from the global network of observatories—INTERMAGNET. We used IMF and solar wind data recorded by instruments aboard ACE satellite. The time-shifted IMF and solar wind data to the nose of the Earth's bow shock are available at http://omniweb.gsfc.nasa.gov/form/.

In this study, we selected non-storm time isolated substorm events to delineate the effect of prompt penetration on the low latitude asymmetry. It is known that intense storms can contribute to asymmetric magnetic field variations in local times (e.g., Singh et al., 2012c, and references therein). Only those durations were considered when $Dst > -60$ nT. We defined isolated substorms as sharp depression in the *AL* index reaching beyond -400 nT from fairly quiet auroral electrojet condition ($AL > -200$ nT) for at least 1 h before the onset of sharp depression. Recovery of substorm was considered when the *AL* index reached to pre-substorm level. It should be noted that there is no well-defined criterion based on the existing auroral electrojet indices for selection of substorms (e.g., Rostoker et al., 1980). We believe that our substorm selection criteria is reasonable in the sense that selected substorms were fairly intense and would produce significant magnetic field variations in the low latitude region. Since the prompt penetration mainly depends upon the IMF *Bz* changes, we consider only those substorm events when (i) changes in *Bz* are smooth, i.e., $\Delta Bz < 5$ nT within 10 min interval and (ii) *Bz* changes are sharp, i.e., $\Delta Bz > 10$ nT (south to north) within 10 min interval. Sharp north to south *Bz* turnings were not considered in this study because such turnings were often found to initiate a series of substorms or intense geomagnetic storms. We discarded cases coinciding with sharp solar wind pressure variations ($\Delta P/P_o > 2$) to avoid the effect of any additional source of low latitude asymmetry. Moreover, it was assured that there were no intense solar flares during selected events as flares could substantially contribute to *ASY* indices.

We visually scanned 3-year interval (2004–2006) data for the selection of events. With the above criteria we found 53 substorm events in the category-1 (i.e., slowly varying IMF *Bz*) and 16 events in category-2 (i.e., sharply varying IMF *Bz* from south to north).

3. Observational results and discussion

In this section, we present a detailed comparative study of these two categories of events and their low latitude magnetic signatures. The last part of the section provides the statistical studies of these two types of substorm events.

3.1. Substorm events of January 2, 2005

A high-speed (~ 700 km/s) stream of solar wind had hit the Earth's magnetosphere during early hours of January 2, 2005 and continued over next several days. The north–south component of IMF (*Bz*), believed to play the most dominant role in the geo-effectiveness (Dungey, 1961; Gonzalez et al., 1994), kept on fluctuating between north and south (mainly between -10 and $+10$ nT) and did not produce major storm. However, many intense substorm activities were evident in the *AL* index during the day. Interestingly, we could identify two different substorms in the two categories described above on this day.

Fig. 1 illustrates the IMF, solar wind conditions and geomagnetic activity indices during 12:30–23:00 UT on January 2, 2005. Two intense substorms are evident in the figure as marked by events A and B between pairs of dashed vertical lines. The minimum *AL* values for events A and B are around –1500 nT and –1000 nT, respectively. Event *A* started around 13:40 UT with moderate but sharp depression in *AL* which later intensified to ~ -1500 nT when IMF *Bz* turned southward at ~ 14:50 UT. Solar wind density (*Nsw*), dynamic pressure (*Psw*) and velocity (*Vsw*) do not exhibit significant change during the event A. The substorm A recovered after 18:30 UT. Another major intensification of westward electrojet (event B) started around 20:15 UT following southward turning of IMF *Bz*. During the expansion phase of this substorm, two sharp IMF *Bz* fluctuations from south to north (>10 nT) are evident. First *Bz* fluctuation ($\sim 21:00$ UT) was transient and short-lived in the north direction, whereas second fluctuation (after ~ 20 min) was further intense and mostly stayed northward after turning from south. The second IMF *Bz* fluctuation was accompanied by a moderate pressure pulse ($\Delta P/P_o \simeq 1.8$).

In Fig. 1, second panel from the bottom shows the low latitude asymmetry indices (*ASYH* and *ASYD*) during the events. It is quite evident that intensification of auroral electrojet is accompanied by low latitude asymmetry enhancement for both the events, A and B. Intensity of the westward electrojet is higher for the event A than that for the event B, but interestingly the *ASYH* is higher for the weaker substorm (event B). There is no major difference in *ASYD* values for the two events. Bottom panel of Fig. 1 shows the *Dst* index which represents the intensity of the ring current. *Dst* values indicates a weak magnetic storm on the day (minimum $Dst \sim -50$ nT).

To bring out differences in the *AL* and *ASY* values more clearly for the two substorm events, we depict the scatter between the magnitude of *AL* index (i.e., $|AL|$) and *ASYH/D* index for events A and B in Fig. 2. The left panel shows the scatter between $|AL|$ and *ASYH* (open and filled circles represent events A and B, respectively), whereas the right panel shows the same between $|AL|$ and *ASYD*. It should be noted that the $|AL|$ index is higher for the substorm A (minimum $AL \sim -1500$ nT) than that for the substorm B (minimum $AL \sim -1000$ nT). But scatter plot (Fig. 2a) shows that the *ASYH* is significantly higher for event B (filled circles) than those for event A (open circles). As seen in Fig. 2a, robust fit for the event B scatter plot (shown by thick line) is much steeper than that for event A (shown by thin line).

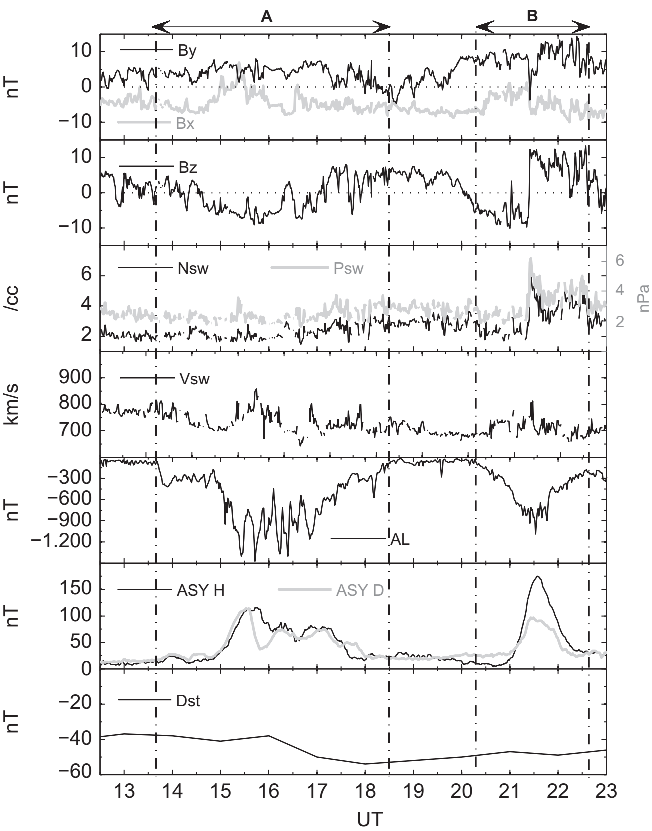

Fig. 1. IMF, solar wind conditions and geomagnetic indices on January 2, 2005. First two panels from the top show components of IMF, whereas *Psw*, *Nsw* and *Vsw* are given in next two panels. Two different intensifications of auroral electrojets, events A and B, marked between pairs of vertical lines show clear *ASYH/D* enhancements. IMF *Bz* is slowly varying during event A than that during event B. *Dst* index is shown in the bottom panel of the figure.

Table 1
List of low-/mid-latitude INTERMAGNET stations, their geographic and geomagnetic coordinates (Epoch-2005).

Station name	Code	Geographic		Geomagnetic	
		Lat. (°N)	Long. (°E)	Lat. (°N)	Long. (°E)
Hermanus	HER	−34.4	19.2	−33.8	84.1
Qsaybeh	QSB	33.9	35.6	30.1	113.4
Alibag	ABG	18.6	72.9	10.0	146.2
Amsterdam	AMS	−37.8	77.6	−46.2	144.4
Zhaoqing	GZH	23.0	112.4	12.6	176.0
Memambetsu	MMB	43.9	144.2	35.16	148.68
Honolulu	HON	21.3	202.0	21.5	269.8
Tucson	TUC	32.2	249.3	39.7	43.8
Stennis	BSL	30.4	270.6	40.0	340.1
San Juan	SJG	18.1	293.8	28.2	6.1
Guimar-Tenerife	GUI	28.3	343.6	33.6	60.6

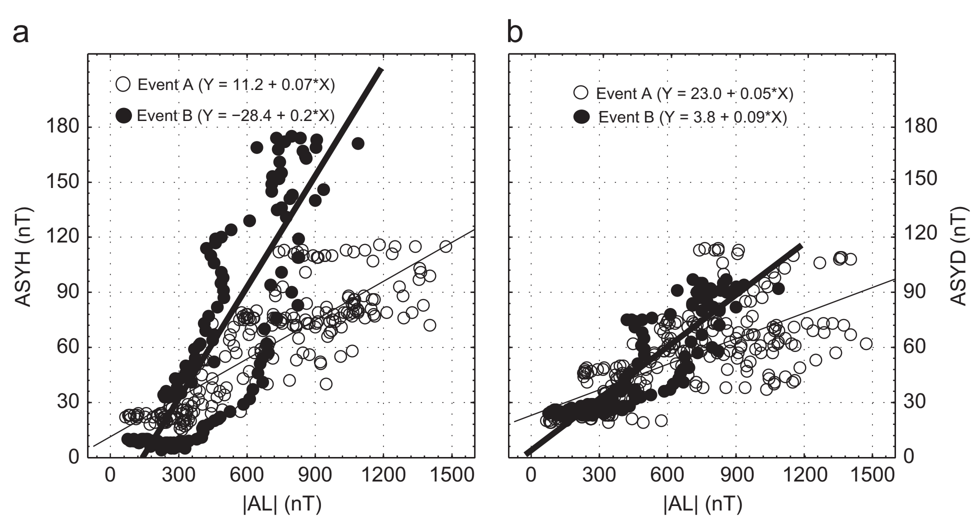

Fig. 2. Scatter plot of $|AL|$ vs *ASYH/D* for events A and B. (a) Open circles show $|AL|$ vs *ASYH* during event A, whereas the filled circles show the same for event B. Thin and thick lines show robust fit for events A and B, respectively. (b) Same as (a) but for $|AL|$ vs *ASYD*.

It is clearly evident from Fig. 2a that the low latitude *ASYH* is higher during sharply changing IMF *Bz* condition (event B) than that during comparatively slowly varying *Bz* condition (event A). *ASYD* vs $|AL|$ scatter as seen in Fig. 2b for events A and B are almost similar, however, robust fit during event B (thick line) shows slightly steeper response than that for event A (thin line).

It is known that low latitude magnetic signature of a substorm depends upon local time of the observatory. Here, we examine signatures of substorms, observed on January 2, 2005, by taking data from various closely spaced low latitude stations (listed in Table 1) distributed around the globe. It will help us to understand which local time contributed towards higher asymmetry during a weaker substorm. Fig. 3a and b respectively show *H* and *D* component disturbances (thick lines) during 13:00–23:00 UT on January 2, 2005, after subtracting the quiet day curve. The *H* and *D* quiet day curves for individual stations were calculated by taking an average of respective data on five international quietest days of the month provided by WDC, Kyoto. Codes of stations are given between the two plots. The *H* disturbance at each of the stations is divided by $\cos(\theta)$ (where θ is the average magnetic latitude of observatories) for latitude correction (Iyemori and Rao, 1996). The two events, A and B, are marked between pairs of dotted vertical lines. Local times at different stations are displayed in figures at the onset of events.

Observatories on the night side of the Earth show positive bay in *H* (thick lines) during substorms A and B, whereas those on the dayside witness depression in *H*, more clearly and sharply during the event B (see Fig. 3a). It is shown in the bottom panel of Fig. 3a that a weak storm (*SYMH* ~ -50 nT) was in progress during the events. Therefore, *H* disturbance at stations away from the substorm current wedge could be dominated by the global ring current or processes going on the dayside of the Earth. Variations in the *D* component are expected to be minimum near the center of substorm current wedge and increase/decrease in dusk/dawn side (McPherron et al., 1973b). It is not very clear during the substorm A which exhibits multiple intensifications, however, during the event B variation in *D* (thick lines in Fig. 3b) is fairly small near midnight and increases towards dusk, whereas decreases towards dawn. *D* disturbances on the dayside are fairly small as shown in Fig. 3b.

Averages of *H* and *D* disturbances, observed at globally distributed 11 stations, are depicted in the bottom panels of Fig. 3a and b, respectively. It is evident that the short scale fluctuations in *SYMH*-11 and *SYMD*-11 are fairly subsided due to averaging. Here *SYMH*/*D*-11 stands for the equivalent *SYMH*/*D* index derived using data from 11 stations. Thin lines in upper panels of Fig. 3a and b respectively show asymmetric *H* and *D* variations at individual stations, which are obtained by subtracting the *SYMH*-11/*SYMD*-11 from the *H*/*D* disturbance at respective stations. Variations of asymmetric *H* or *D*

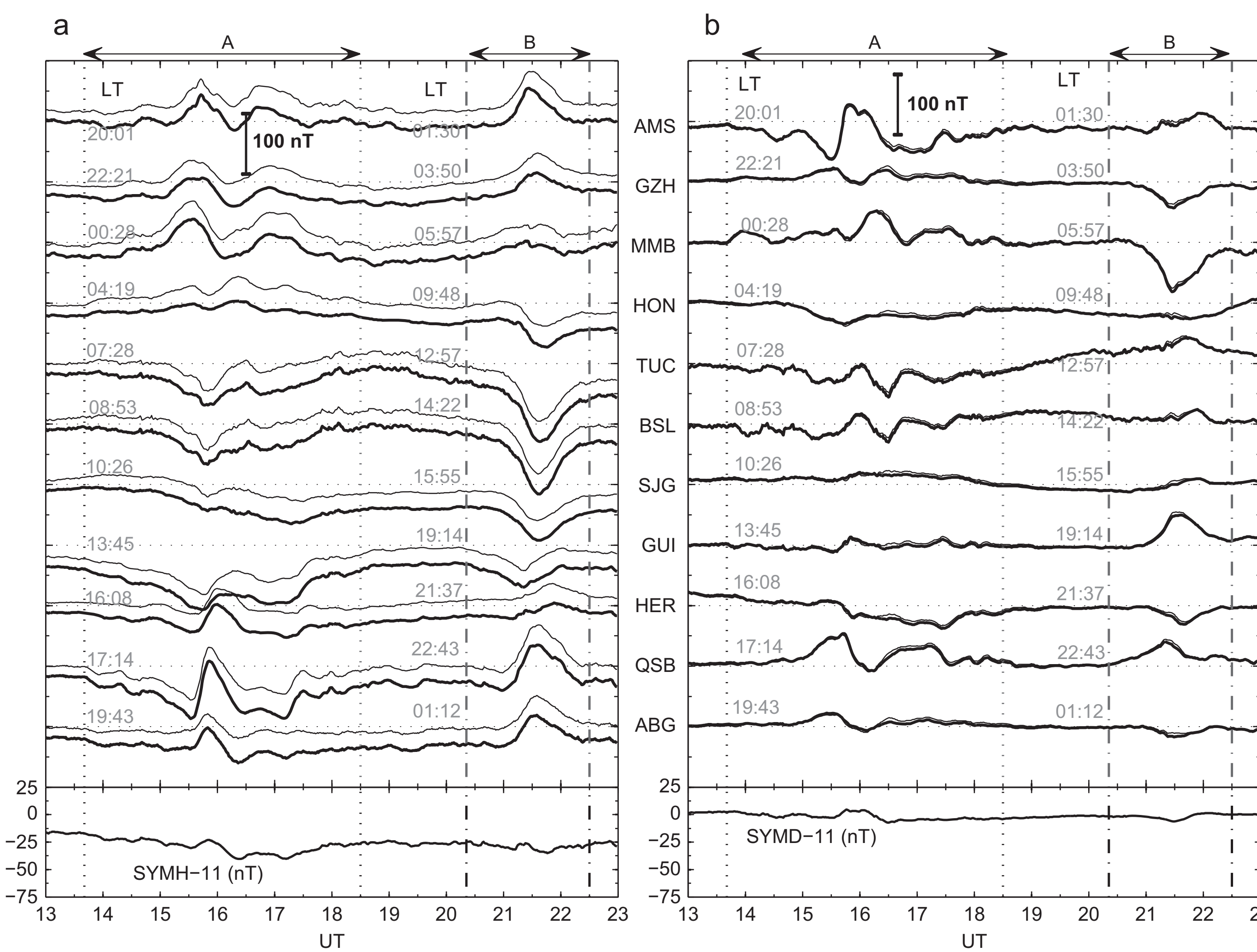

Fig. 3. (a) *H* disturbance at longitudinally distributed low-/mid-latitude stations are shown by thick lines in the upper panel. Averaged *H* disturbance, i.e., equivalent *SYMH* is shown in the bottom panel of the figure. Asymmetry in *H* at corresponding station is plotted by thin line. Local times at different stations are marked in plot at the onset of events. (b) Same as (a) but for *D* disturbance.

at individual stations are grossly similar to the *H* or *D* component disturbances except for the fact that asymmetry in *H* is shifted positively. The asymmetric time series can be used to derive the *ASY* index which is difference between the maximum and minimum of all time series at each instant of time.

The additional enhancement in *ASYH* during event B coincided with the sharp IMF *Bz* orientation change. It is expected that the sharp IMF *Bz* turning from south to north produces a westward electric field on the dayside, which in turn depresses *H* component. As shown in Fig. 3a, stations on the dayside of the Earth witness sharp depression in the *H* component during the event B. Thus, sharp IMF *Bz* orientation change will be an additional feed for low latitude asymmetry, especially in the *H* component.

It should be noted that the sharp IMF *Bz* traversal from south to north was accompanied by a small pressure pulse (see Fig. 1). Shi et al. (2005) pointed out that the pressure pulses can further intensify the ring current asymmetry provided that the ring current is already asymmetric. However, the pressure pulse shown in Fig. 1 is not so intense and initiation of asymmetric enhancement slightly prior to pressure pulse is associated with the substorm activity, not the ring current asymmetry.

In Fig. 4, we show an example when a pressure pulse of similar magnitude ($\Delta P/P_o \simeq 1.6$) was observed during quiet magnetic condition on January 24, 2006. It is seen that the pressure enhancement does not affect the asymmetric indices (*ASYH*/*D*), however, clear enhancement in *SYMH* is observed (bottom panel of Fig. 4). *SYMH* index is essentially the 1-min resolution version of hourly *Dst* index (Iyemori and Rao, 1996). This pressure pulse resulted in enhanced *H* field in different local times including the dayside (not shown here).

It is well known that pressure enhancement intensifies the magnetopause current, which is identified as positive perturbation in *H* component at the ground (Araki, 1977). Fig. 3 shows that the *H* component on the dayside is depressed for both events A and B (very sharply for event B). For event B, due to pressure pulse one would expect enhanced *H* field at stations located on the dayside (away from substorm current wedge). On the contrary, the depression in *H* is observed more prominent for event B than that for event A due to penetration of IEF associated with sharp IMF *Bz* orientation change. The intensified ring current will depress the *H* field globally, however, role of the ionospheric electric field associated with sharp traversal of IMF *Bz* from south to north is clearly seen in the dayside magnetic field variations. The prompt penetration of electric field resulted in higher asymmetry at low-/mid-latitudes during a weaker substorm.

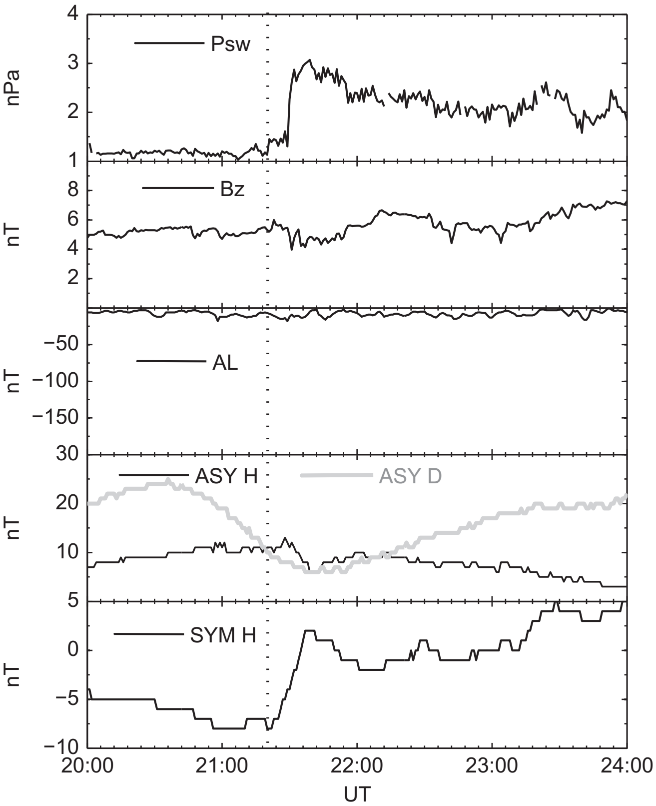

Fig. 4. A typical example showing effect of pressure pulse on *SYM* and *ASY* indices on a magnetically quiet day January 24, 2006. From top to bottom *Psw*, IMF *Bz*, *AL*, *ASYH*/*D* and *SYMH* indices are shown. Effect of pressure enhancement is evident in *SYMH*, while *ASY* indices remain unaffected.

3.2. Statistical results

In order to establish clear role of IMF *Bz* orientation change on the low latitude asymmetry, we divided isolated substorm events into two categories, viz. slowly and sharply varying IMF *Bz* as

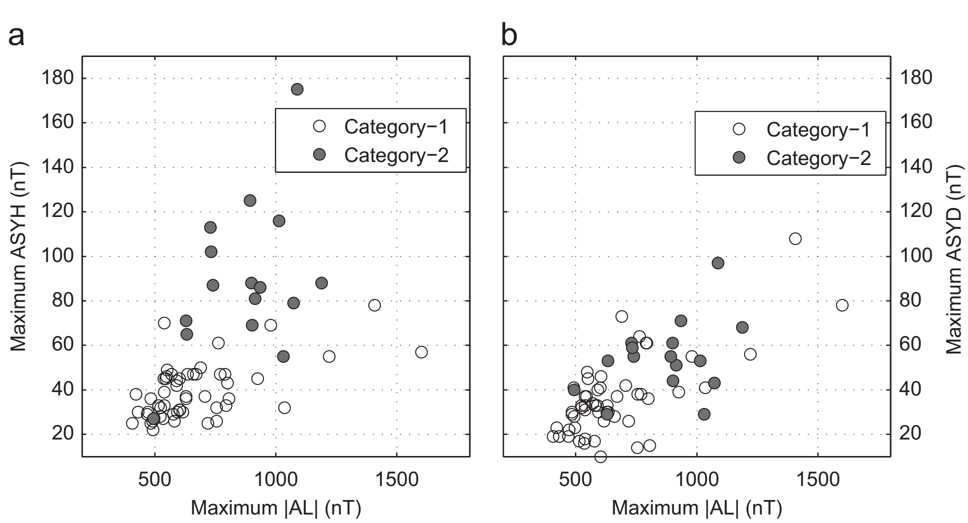

Fig. 5. Scatter plot of the maximum $|AL|$ vs maximum *ASYH*/*D* for the two categories of substorm events selected during year 2004–2006. (a) Scatter plot for slowly and sharply varying IMF *Bz* conditions (category-1 and category-2, respectively) are shown by open and filled circles, respectively. (b) Same as (a) but for the maximum $|AL|$ vs maximum *ASYD*. *ASYH* values are significantly higher during sharp IMF *Bz* orientation changes in figure (a), whereas no such clear enhancement is evident for *ASYD*.

discussed in Section 2. We found 53 and 16 events, respectively under slowly varying *Bz* condition (category-1) and sharply varying *Bz* condition (category-2). Fig. 5 shows the scatter plot between $|AL|$ and $ASYH/D$ indices for events in category-1 (open circles) and events in category-2 (filled circles). Each point in the figure represents the magnitude of the minimum value of *AL* index on the *X*-axis and the maximum value of $ASYH/D$ on the *Y*-axis for different selected substorm events. It is evident from Fig. 5a that the *ASYH* is significantly higher for substorms triggered during sharply varying IMF *Bz* conditions (filled circles) than those triggered during slowly varying IMF *Bz* (open circles). However, we do not see clear difference in *ASYD* for the two categories of substorm events (Fig. 5b). It is expected that the promptly penetrated zonal electric field will predominantly affect *H* component, whereas *D* component remains almost unaffected (Abdu et al., 2007).

4. Summary and conclusion

Geomagnetic substorms make substantial changes in the magnetic field right from high to low latitudes on the Earth's surface. The standard *AL* and $ASYH/D$ are widely used for identification of substorms. However, there are subtle differences between *AL* and *ASY* indices. The *AL* index represents the maximum intensity of the westward auroral electrojet which is closely related to substorm onset on the nightside. At low latitudes, magnetic disturbance on the nightside is dominated by substorm current wedge, whereas on the dayside of the Earth various ionospheric currents influence the magnetic field variations. The *ASY* indices, derived using data from low latitude stations distributed in local time, are likely to be affected by processes other than substorms.

In this study, we performed a statistical study of substorm-time *AL* and $ASYH/D$ indices during slowly and sharply varying IMF *Bz* conditions. The important findings of this study are listed below

1. Sharp IMF *Bz* changes from south to north during substorms could result in the penetration of IEF to the lower latitudes. The IEF can drive intense westward ionospheric current on the dayside (due to high conductivity) causing a substantial depression in the *H* field. The nightside magnetic field remains almost unaffected by the IEF due to low ionospheric conductivity.
2. IMF *Bz* orientation changes during substorms become an additional source of asymmetry at low latitudes, which intensifies particularly *ASYH* index. However, the zonal electric field associated with the penetration of IEF does not produce significant change in *ASYD*.

Acknowledgments

Authors thank OMNIWeb (http://omniweb.gsfc.nasa.gov/) for providing time-shifted interplanetary observations and World Data Center, Kyoto (http://wdc.kugi.kyoto-u.ac.jp/) for geomagnetic indices. Global ground magnetic field data taken from INTERMAGNET (www.intermagnet.org) is sincerely acknowledged.

References

Abdu, M.A., Jayachandran, P.T., MacDougall, J., Cecile, J.F., Sobral, J.H.A., 1998. Equatorial F region zonal plasma irregularity drifts under magnetospheric disturbances. Geophysical Research Letters 25, 4137–4140.

Abdu, M.A., Maruyama, T., Batista, I.S., Saito, S., Nakamura, M., 2007. Ionospheric responses to the October 2003 superstorm: longitude/local time effects over equatorial low and middle latitudes. Journal of Geophysical Research 112, A10306, http://dx.doi.org/10.1029/2006JA012228.

Akasofu, S.-I., 1981. Energy coupling between the solar wind and the magnetosphere. Space Science Reviews 28, 121–190, http://dx.doi.org/10.1007/BF00218810.

Araki, T., 1977. Global structure of geomagnetic sudden commencement. Planetary and Space Science 25, 373–384.

Baumjohann, W., Treumann, R.A., 1997. Basic Space Plasma Physics. Springer, New York.

Caan, M., McPherron, R.L., Russell, C.T., 1975. Substorm and interplanetary magnetic field effects on the geomagnetic tail lobes. Journal of Geophysical Research 80, 191–194.

Crooker, N.C., 1972. High-time resolution of the low-latitude asymmetric disturbance in the geomagnetic field. Journal of Geophysical Research 77, 773–775.

Davis, T., Sugiura, M., 1966. Auroral electrojet activity index AE and its universal time variations. Journal of Geophysical Research 71, 785–801.

Dungey, J.W., 1961. Interplanetary magnetic field and the auroral zones. Physical Review Letters 6, 47–49.

Fejer, B.G., Gonzales, C.A., Farley, D.T., Kelley, M.C., Woodman, R.F., 1979. Equatorial electric fields during magnetically disturbed conditions, 1. The effect of the interplanetary magnetic field. Journal of Geophysical Research 84, 5797–5802.

Gonzales, C.A., Kelley, M.C., Fejer, B.G., Vickrey, J.F., Woodman, R.F., 1979. Equatorial electric fields during magnetically disturbed conditions, 2. Implications of simultaneous auroral and equatorial measurements. Journal of Geophysical Research 84, 5803–5812.

Gonzalez, W.D., Joselyn, J.A., Kamide, Y., Kroehl, H.W., Rostoker, G., Tsurutani, B.T., Vasyliunas, V.M., 1994. What is a geomagnetic storm? Journal of Geophysical Research 99, 5771–5792.

Grafe, A., Bespalov, P.A., Trakhtengerts, V.Y., Demekhov, A.G., 1997. Afternoon mid-latitude current system and low-latitude geomagnetic field asymmetry during geomagnetic storms. Annales Geophysicale 15, 1537–1547.

Hamilton, D.C., Gloeckler, G., Ipavich, F.M., Studemann, W., Wilken, B., Kremser, G., 1988. Ring current development during the great geomagnetic storm of February 1986. Journal of Geophysical Research 93, 14343–14355.

Henderson, M., Reeves, G., Belian, R., Murphree, J., 1996. Observations of magnetospheric substorms occurring with no apparent solar wind/IMF trigger. Journal of Geophysical Research 101, 10773–10791.

Hsu, T.S., McPherron, R.L., 2004. Average characteristics of triggered and non-triggered substorms. Journal of Geophysical Research 109, A07208, http://dx.doi.org/10.1029/2003JA009933.

Hsu, T.-S., McPherron, R.L., 2009. A statistical study of the spatial structure of interplanetary magnetic field substorm triggers and their associated magnetic response. Journal of Geophysical Research 114, A02223, http://dx.doi.org/10.1029/2008JA013439.

Huang, C.-S., Foster, J.C., Goncharenko, L.P., Reeves, G.D., Chau, J.L., Yumoto, K., Kitamura, K., 2004. Variations of low-latitude geomagnetic fields and Dst index caused by magnetospheric substorms. Journal of Geophysical Research 109, A05219, http://dx.doi.org/10.1029/2003JA010334.

Huang, C.-S., Foster, J.C., Kelley, M.C., 2005. Long-duration penetration of the interplanetary electric field to the low-latitude ionosphere during the main phase of magnetic storms. Journal of Geophysical Research 110, A11309, http://dx.doi.org/10.1029/2005JA011202.

Iyemori, T., Rao, D.R.K., 1996. Decay of the Dst field of geomagnetic disturbance after substorm onset and its implication to storm–substorm relation. Annales Geophysicae 14, 608–618.

Kamide, Y., Rostoker, G., 2004. What is the physical meaning of the AE index? EOS Transactions AGU 85, 188–192.

Kelley, M.C., Fejer, B.G., Gonzales, C.A., 1979. An explanation for anomalous equatorial ionospheric electric fields associated with a northward turning of the interplanetary magnetic field. Geophysical Research Letters 6, 301–304.

Kikuchi, T., Araki, T., 1979. Horizontal transmission of the polar electric field to the equator. Journal of Atmospheric Terrestrial Physics 41, 927–936.

Kikuchi, T., Lühr, H., Schlegel, K., Tachihara, H., Shinohara, M., Kitamura, T.-I., 2000. Penetration of auroral electric fields to the equator during a substorm. Journal of Geophysical Research 105, 23251–23261.

Kokubun, S., McPherron, R.L., Russell, C.T., 1977. Triggering of substorms by solar wind discontinuities. Journal of Geophysical Research 82, 74–86.

Liemohn, M., Kozyra, J., Thomsen, M., Roeder, J., Lu, G., Borovsky, J., Cayton, T., 2001. Dominant role of the asymmetric ring current in producing the stormtime Dst*. Journal of Geophysical Research 106, 10,883–10,904.

Liu, J.-M., Zhang, B.-C., Kamide, Y., Wu, Z.-S., Hu, Z.-J., Yang, H.-G., 2011. Spontaneous and trigger-associated substorms compared: electrodynamic parameters in the polar ionosphere. Journal of Geophysical Research 116, A01207, http://dx.doi.org/10.1029/2010JA015773.

Lui, A., 2004. Potential plasma instabilities for substorm expansion onsets. Space Science Reviews 113, 127–206.

Lyons, L., 1996. Substorms: fundamental observational features, distinction from other disturbances, and external triggering. Journal of Geophysical Research 101, 13011–13025.

Lyons, L., Blanchard, G.T., Samson, J.C., Lepping, R.P., Yamamoto, T., Moretto, T., 1997. Coordinated observations demonstrating external substorm triggering. Journal of Geophysical Research 102, 27,039–27,051.

McPherron, R.L., Russell, C.T., Aubry, M.P., 1973a. Satellite studies of magnetospheric substorms on August 15, 1968: 9. Phenomenological model for substorms. Journal of Geophysical Research 78, 3131–3149.
McPherron, R.L., Russell, C.T., Kivelson, M., Coleman, P., 1973b. Substorms in space: the correlation between ground and satellite observations of the magnetic field. Radio Science 8, 1059–1076.
Nishida, A., 1968. Coherence of geomagnetic DP 2 fluctuations with interplanetary magnetic variations. Journal of Geophysical Research 73, 5549–5559.
Rastogi, R.G., Janardhan, P., Ahmed, K., Das, A.C., Bisoi, S.K., 2010. Unique observations of a geomagnetic SI^{+}–SI^{-} pair: solar sources and associated solar wind fluctuations. Journal of Geophysical Research 115, A12110, http://dx.doi.org/10.1029/2010JA015708.
Rostoker, G., Akasofu, S.-I., Foster, J., Greenwald, R., Kamide, Y., Kawasaki, K., Lui, A., McPherron, R.L., Russell, C.T., 1980. Magnetospheric substorms-definition and signatures. Journal of Geophysical Research 85, 1663–1668.
Sastri, J., Abdu, M.A., Sobral, J.H.A., 1997. Response of equatorial ionosphere to episodes of asymmetric ring current activity. Annales Geophysicae 15, 1316–1323.
Sastri, J., Rao, J., Rao, D., Pathan, B.M., 2001. Daytime equatorial geomagnetic H field response to the growth phase and expansion phase onset of isolated substorms: case studies and their implications. Journal of Geophysical Research 106, 29925–29933.
Sastri, J.H., 2002. Equatorial geomagnetic and ionospheric effects of substorms. Indian Journal of Radio and Space Physics 31, 309–320.
Shi, Y., Zesta, E., Lyons, L.R., Boudouridis, A., Yumoto, K., Kitamura, K., 2005. Effect of solar wind pressure enhancements on storm time ring current asymmetry. Journal of Geophysical Research 110, A10205, http://dx.doi.org/10.1029/2005JA011019.
Shi, Y., Zesta, E., Lyons, L.R., Yumoto, K., Kitamura, K., 2006. Statistical study of effect of solar wind pressure enhancements on dawn-to-dusk ring current asymmetry. Journal of Geophysical Research 111, A10216, http://dx.doi.org/10.1029/2005JA011532.
Singh, A.K., Jayashree, B., Sinha, A.K., Rawat, R., Pathan, B.M., Dhar, A., 2011. Observations of near-conjugate high latitude substorms and their low latitude implications. Current Science 101, 1073–1078.
Singh, A.K., Sinha, A.K., Rawat, R., Jayashree, B., Pathan, B.M., Dhar, A., 2012a. A broad climatology of very high latitude substorms. Advances in Space Research 50, 1512–1523.
Singh, A.K., Sinha, A.K., Pathan, B.M., Rawat, R., 2012b. Solar flare effect on low latitude ASY indices. Journal of Atmospheric and Solar–Terrestrial Physics 77, 119–124.
Singh, A.K., Sinha, A.K., Rajaram, R., Pathan, B.M., 2012c. Storm-time longitudinally propagating asymmetric modes at low latitudes. Annales Geophysicae 30, 131–141, http://dx.doi.org/10.5194/angeo-30-131-2012.
Sobral, J.H.A., Abdu, M.A., González, W.D., Tsurutani, B.T., Batista, I.S., González, A.L., 1997. Effects of intense storms and substorms on the equatorial ionosphere/thermospheres system in the American sector from ground-based and satellite data. Journal of Geophysical Research 102, 14305–14313.
Troshichev, O.A., Kotikov, A.L., Bolotinskaya, B.D., Andrezen, V.G., 1986. Influence of the IMF azimuthal component on magnetospheric substorm dynamics. Journal of Geomagnetism and Geoelectricity 38, 1075–1088.
Veenadhari, B., Alex, S., Kikuchi, T., Shinbori, A., Singh, R., Chandrasekhar, E., 2010. Penetration of magnetospheric electric fields to the equator and their effects on the low-latitude ionosphere during intense geomagnetic storms. Journal of Geophysical Research 115, A03305, http://dx.doi.org/10.1029/2009JA014562.
Wada, T., Iyemori, T., Nose, M., 1998. Automated detection of substorm onsets by several independent methods. In: Kokunun, S., Kamide, Y. (Eds.), Substorm-4. Terra Scientific Publishing Company, Japan, pp. 379–382.